energies

MDPI

Review

A Review of Experimental and Numerical Analyses of Solar Thermal Walls

Krzysztof Sornek [1,*], Karolina Papis-Frączek [1], Francesco Calise [2], Francesco Liberato Cappiello [2] and Maria Vicidomini [2]

[1] Department of Sustainable Energy Development, Faculty of Energy and Fuels, AGH University of Science and Technology, Mickiewicza Ave. 30, 30-059 Krakow, Poland; papis@agh.edu.pl
[2] Department of Industrial Engineering, University of Naples Federico II, P.le Tecchio 80, 80125 Naples, Italy; frcalise@unina.it (F.C.); francescoliberato.cappiello@unina.it (F.L.C.); maria.vicidomini@unina.it (M.V.)
* Correspondence: ksornek@agh.edu.pl

Abstract: Nowadays, almost 30% of total energy consumption (130 EJ) is consumed for the operation of buildings, mainly by space heating/cooling and ventilation systems, hot water preparation systems, lighting, and other domestic appliances. To improve the energy efficiency of buildings, several countries are promoting the use of renewable energy. The most promising systems include active and passive solar installations. In passive systems, the solar energy is collected, stored, reflected, or distributed by the roof ponds, natural convective loops, and the most popular direct gain walls and thermal storage walls (known as Trombe walls). This paper reviews the experimental and numerical studies devoted to the different solutions of Trombe walls, including solar chimneys integrated on the vertical walls, classic Trombe walls, Trombe walls with incorporated phase change materials, and photovoltaic Trombe walls. The actual state of the art is presented in the context of reducing energy consumption and enhancing thermal comfort. Most of the analyzed studies showed that the application of thermal storage walls allowed achieving these goals, led to lower emissions of greenhouse gases, and improved living standards. Nevertheless, there is a need for more detailed feasibility studies, including cost and environmental indicators.

Keywords: nearly zero energy buildings; passive solar systems; solar energy; solar air heaters; solar thermal walls; solar chimneys

Citation: Sornek, K.; Papis-Frączek, K.; Calise, F.; Cappiello, F.L.; Vicidomini, M. A Review of Experimental and Numerical Analyses of Solar Thermal Walls. *Energies* **2023**, *16*, 3102. https://doi.org/10.3390/en16073102

Academic Editors: Constantinos A. Balaras and Tomasz Cholewa

Received: 17 February 2023
Revised: 24 March 2023
Accepted: 27 March 2023
Published: 29 March 2023

1. Introduction

Nowadays, almost 130 EJ of energy is consumed per year for the operation of buildings. This amount accounts for 30% of total energy consumption. Moreover, the construction services sector uses an additional 21 EJ of energy [1]. The most significant share in this sector, almost 70%, belongs to residential buildings. In such buildings, energy is mainly consumed for heating, ventilation, air conditioning (HVAC), hot water preparation systems, and other domestic appliances [2,3]. Developing and introducing innovative solutions that can provide higher energy performance for buildings is essential to making these systems more energy-efficient and reducing their carbon footprint. An example of buildings that minimize or even totally eliminate negative impacts on climate and the natural environment in their design, construction, and operation are net-zero energy buildings (NZEBs). NZEBs are characterized by several features, including:

- Excellent thermophysical properties (transmittance, mass, g-value, etc.) of the building envelope, including roofs, walls, windows, doors, etc.;
- The efficient usage of natural resources;
- The use of clean energy, including renewable energy sources;
- The reduction of pollution and waste generation by means of reusing and recycling;
- Good indoor air quality [4,5].

The development of NZEBs can be realized in different ways. One of the available options is the use of the Trias Energetica strategy. The three elements of the Trias Energetica strategy are:

- Reduce the demand for primary energy;
- The use of renewable energy sources;
- If fossil fuels are still needed, use them as efficiently and cleanly as possible [6,7].

This approach is useful; however, the most detailed energy-saving pyramid can be considered. An example of a 5-step energy-saving pyramid is shown in Figure 1.

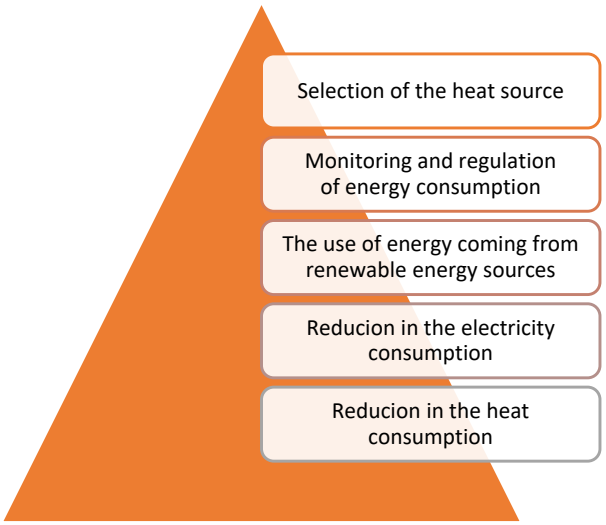

Figure 1. An example of a 5-step energy-saving pyramid.

As shown in Figure 1, reducing heat and electricity consumption from traditional sources and using renewable energy is crucial from the standpoint of energy efficiency in buildings. Among other renewable energy sources, solar energy is considered one of the most promising options. It is commonly used for electricity production (photovoltaic systems), supplying heat and hot water production (solar-thermal systems), and also for cooling buildings [8,9]. Solar energy can fully or partially fulfill the heating demands of residential buildings. In the 1930s, in the United States, the idea of "solar houses" became popular. Firstly, these solar houses were characterized by large, south-facing windows that collected more sun rays during winter [10]. Actually, solar energy can be utilized in buildings in two types of systems:

- Active solar energy (ASE) systems require external energy sources to power blowers, pumps, etc. to collect, store, and convert solar energy. ASE includes systems equipped with solar thermal collectors [11], photovoltaic panels (PV) [12], photovoltaic thermal collectors (PV/T) [13], concentrated photovoltaic (CPV) [14,15], concentrated photovoltaic thermal (CPV/T) [16], hybrid installations [17,18], etc.;
- Passive solar energy (PSE) systems collect, store, and distribute solar energy using conventional building elements. Passive strategies fulfill the heating, cooling, and lighting needs, so they can be implemented in residential and nonresidential buildings [19].

Various passive technologies selectively harness solar energy to heat a building without using (or significantly reducing the use of) typical heaters powered by fossil fuels. Passive solar buildings are designed to use common construction elements (such as walls, floors, roofs, and windows) in energy applications. They collect solar radiation, then store it in the form of heat, and finally release energy for heating or cooling purposes (during the winter and summer, respectively). In practice, PSE systems can be realized as the following options:

- The direct-gain installation—which includes large areas of glazing on the south-facing walls—increases the amount of solar energy accumulated by the masonry floors and walls. These massive construction elements store the solar heat, which is gradually released to the house interior during the night;
- The thermal storage wall, specifically the Trombe wall (TW), includes massive external walls that absorb solar energy and then store it; TW may also work in cooling mode [20];
- The solar greenhouse—this construction combines the advantages of the two previously mentioned systems. The most beneficial location of the greenhouse is on the building's south facade [21];
- The roof pond requires a superficial water reservoir, such as a pond or tank, which has to be placed on a flat roof or platform. To reduce the evaporation rate, the surface of the reservoir must be closed by a transparent sheet of foil, glass, or plastic [22];
- The natural convective loop—this system works as the classic thermosyphon, but instead of water, air is used as the working medium [23,24].

The paper reviews the newest experimental and numerical analyses focused on thermal storage walls (Trombe walls). The main goal of the review is to show the actual state of the art and summarize different solutions for Trombe walls from the standpoint of the possibility of decreasing the annual consumption of primary energy and increasing the level of thermal comfort in the buildings.

2. A Brief Description of the Selected Trombe Wall Configurations

The literature presents a description of several configurations of Trombe walls. The specific designs of TWs depend on geographical latitudes and, consequently, different climatic conditions. A brief description of the selected configurations of TWs is presented below, including the following options: solar chimneys integrated on the vertical wall (SCH), classic Trombe walls (CTW), Trombe walls with incorporated phase change materials (PCMTW), and photovoltaic Trombe walls (PVTW).

2.1. Solar Chimney Integrated on the Vertical Wall

The solar chimney is a basic example of a passive solar system used for ventilation. It is one of the technologies that work on the buoyancy principle. It is typically made of massive construction materials painted black for better solar absorption. It can also be integrated with construction elements, usually walls (see Figure 2). The construction of a solar chimney usually has two openings: one at the bottom and one at the top. The sun's heat warms the air in the SCH, causing it to rise and create a draft, which can ventilate the house interior. The air passes through the room and exits from the top of the chimney. Solar chimneys integrated with the walls can also be used on the roof level [25,26].

2.2. The Classic Trombe Wall

The classic Trombe wall is made of construction materials characterized by great heat capacities, such as bricks, concrete or stone slabs, and raw clay, and covered with vertical glass. The application of glazing, especially the number of glass sheets and their thickness, significantly influences the amount of solar radiation transmitted to the wall and accumulated there [27]. Between the layers of glass and the wall, an air gap is created, which enables the natural circulation of air. The energy is transferred to the house interior mainly by two heat transfer mechanisms: conduction (through the Trombe wall) and convection (using heated air that flows upward due to the buoyancy effect). To increase the amount of collected solar energy, the external surface of the wall is colored black [28,29]. A schematic of a classic Trombe wall is shown in Figure 3.

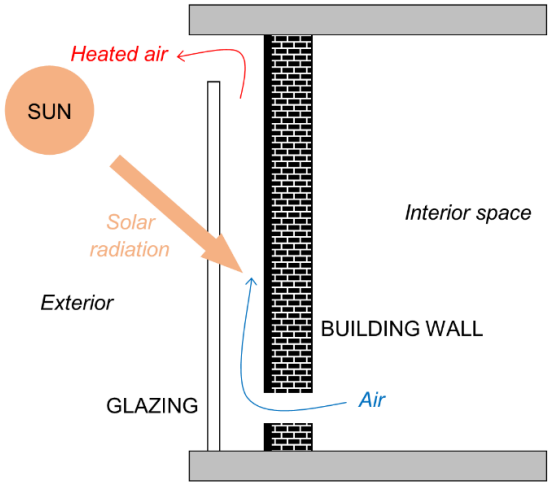

Figure 2. Schematic of a solar chimney integrated on the vertical wall.

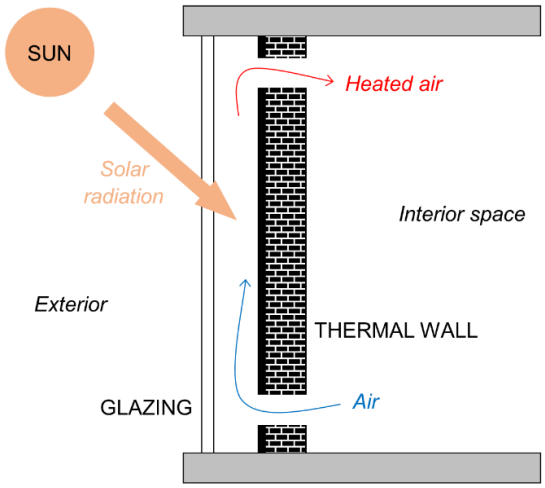

Figure 3. Schematic of a classic Trombe wall.

Based on the ventilation mode of the Trombe wall system, it can be classified into two categories: ventilated and double-ventilated. If openings exist in one wall layer (internal or external), the Trombe wall is classified as ventilated. When vents are present in both system layers, the system is known as double-ventilated [30]. The technology of the classic Trombe wall is considered a beneficial option, especially for private buildings, because of its simple construction and minimal maintenance costs [31].

2.3. The Trombe Wall with Incorporated PCM

The construction of a classic Trombe wall can be upgraded by filling it with phase change materials (PCMs) to enhance the heat gained from solar radiation. It is possible due to PCMs' properties: they can absorb and release large amounts of thermal energy (latent heat) during the melting-solidification process. Moreover, these phase changes occur without a significant increase in temperature [32]. A smaller volume features TWs based on PCM due to the higher thermal capacity of PCM. PCMTWs can also be prefabricated in the factory. Filling the masonry walls with PCMs reduces the temperature fluctuations observed on the inner surface of the Trombe wall. On the other hand, PCMs in Trombe walls are vulnerable to high solar irradiation, which may cause their long-term degradation due to overheating [33,34]. PCM materials are almost invariably rigid, but some flexible, form-stable PCM composites can be obtained by physical mixing and low-temperature curing [35]. Furthermore, to improve the compatibility and performance of PCMs for real-

life building applications, nanotechnology can be incorporated into traditional PCMs [36]. A scheme of a Trombe wall with incorporated PCM is shown in Figure 4.

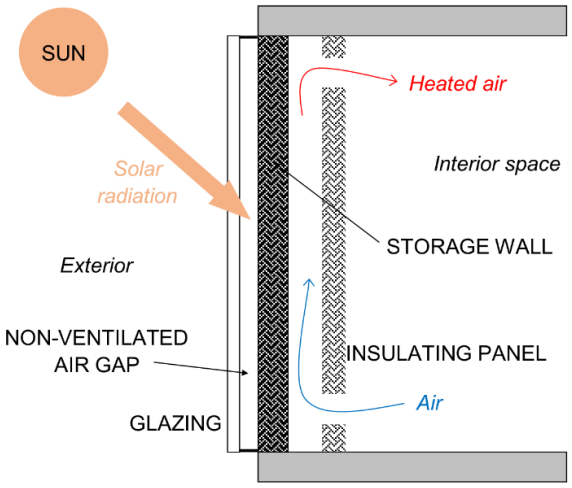

Figure 4. Schematic of a Trombe wall with incorporated PCM.

2.4. The Photovoltaic Trombe Wall

The Trombe wall may also be upgraded by incorporating photovoltaic solar cells. Due to the presence of photovoltaics, the PVTW wall provides not only space heating but also electricity. Moreover, the overall building's aesthetic may be improved in some cases. In general, three configurations of PVTWs are considered. The first one has the solar cells attached to the rear side of the glass sheet (PVGTW), the second configuration incorporates solar cells mounted directly to the outer surface of the massive wall (PVMTW), and the third variant includes the solar cells installed on the blind slats (PVBTW) between the glazing and wall [27,37]. The abovementioned configurations of PVTWs are shown in Figure 5.

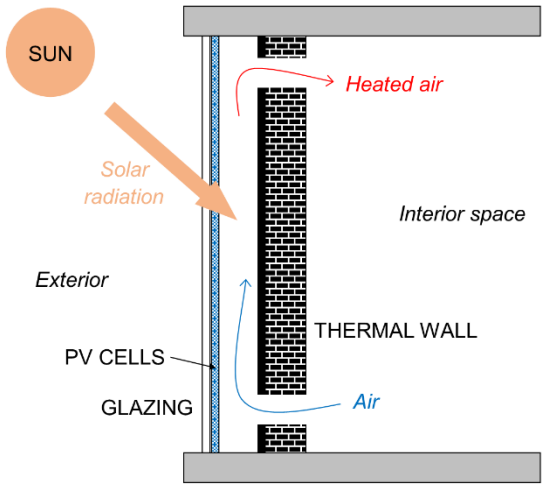

(a)

Figure 5. *Cont.*

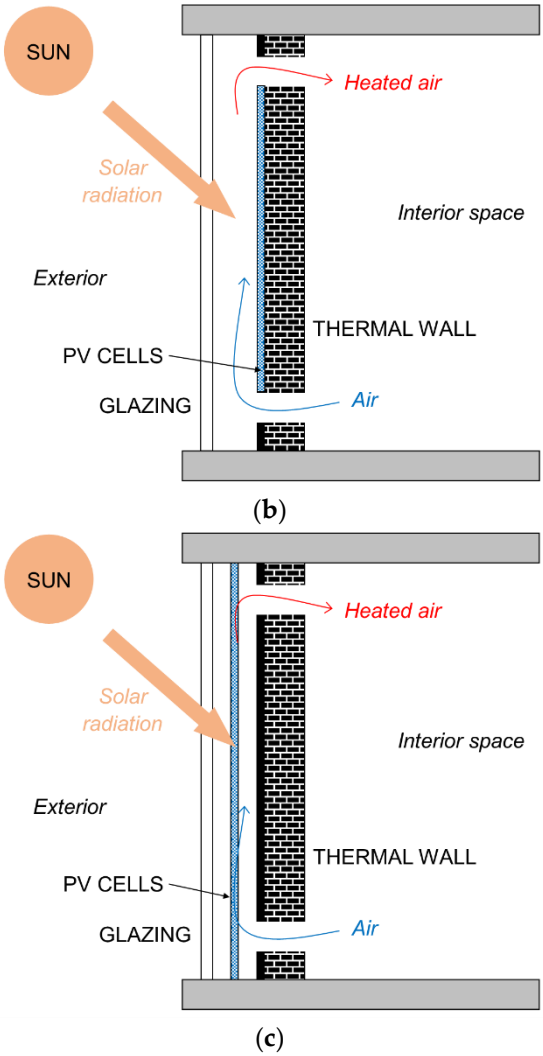

Figure 5. Schematic of a Trombe wall with incorporated photovoltaic solar cells: PVGTW (**a**), PVMTW (**b**), and PVBTW (**c**).

The presence of a glass cover, despite enhancing the thermal gain, significantly increases the temperature of the installed cells and therefore reduces their power [27]. In order to increase the electrical efficiency of photovoltaic cells, active cooling should be provided. The most popular method includes using water or a DC fan.

2.5. Other Designs of Trombe Wall

Apart from SCH, CTW, PCMTW, and PVTW, there are also other designs of specific Trombe walls [38]. These designs may be classified as follows:

- Trombe–Michel wall (TMW)—the wall with insulation added on its inner side. It prevents excessive heat losses from the building to the environment during the night or winter period;
- Water Trombe wall (WTW)—the wall with incorporated internal water reservoirs, which act as additional heat storage;
- Zigzag Trombe wall (ZTW)—a thermal wall characterized by sectional construction. These sections are placed in a characteristic zigzag shape to reduce exposure to solar radiation during the summer months;
- Fluidized Trombe wall (FTW)—the wall with incorporated highly absorptive particles. They are enclosed in the gap created between the wall and the layer of glass.

3. Review of the Selected Trombe Wall Configurations

The abovementioned configurations of the SCHs and TWs have been widely investigated in the literature. The most actual works are presented and summarized below.

3.1. Solar Chimneys Integrated on the Vertical Wall

Due to the depletion of traditional energy sources and their negative influence on the environment, scientists are developing novel energy systems. These issues are also becoming crucial in the field of commercial and domestic building construction. One of the available solutions is to use passive ventilation systems based on solar chimneys [39]. Due to their simplicity and popularity, the SCHs have been thoroughly tested and installed in various buildings. Moreover, mathematical models of the SCHs have been developed to forecast their performance under various operating conditions. Generally, these models are based on detailed energy balance equations specified for each component of the ventilation systems [40,41]. The relationship between the air properties (such as velocity and temperature at the inlet) and the SCH operating parameters for all-year operation has also been discussed [42]. Villar-Ramos et al. [43] evaluated the design, construction, and thermal performance of an SCH under a warm-humid climate. The tested SCH had a length of 2 m and a width of 0.8 m. The authors observed that the maximum temperature difference of 16.7 K was observed for an inclination angle of 15° accompanied by a 0.075-meter air gap. Their research concluded that the airflow in SCH can be increased by up to 5 times with an air change occurring at an hourly rate of 27.1. The influence of the chimney gap size (ranging from 0.1 m to 0.5 m) on the air mass flow rate has been addressed by Hosien and Salim [44]. Results showed that the enlargement of the chimney gap (from 0.1 to 0.5 m) causes a rapid increase in the air flow (from 0.04 to 0.18 kg/s). This means that the gap in the chimney greatly affects the natural ventilation flow rate. Furthermore, Shi et al. [45] summarized four sets of factors that influence the operation of the solar chimney. These factors have been classified as (I) the solar chimney-building configuration, (II) installation methods, (III) the properties of construction materials, and (IV) the impact of the environment. The authors concluded that the most promising and effective way to improve performance is to change the system's configuration. Moreover, it was stated that the continuous development of new materials also positively affects the thermal properties and enhances the operation of solar chimneys. Zhang et al. [46] analyzed the airflow inside a solar chimney, taking into consideration various configurations of the chimney and the tested building. Their study also included the impact of various environmental conditions (e.g., insolation). The SCH's essential configurations and building layout configurations were determined based on the air flow rate and the flow patterns caused by natural convection. The increase in SCH height from 3.0 to 5.0 m enhanced ventilation capacity by 90%. The modification of the air inlet location toward the upper side of the solar chimney resulted in a 57% improvement in the ventilation rate. The application of SCH to smoke exhaustion was explored by Cheng et al. [47] The authors optimized the construction and operation of a solar chimney under natural ventilation and smoke exhaustion conditions with a triple reduction of the scale. Scientists took into consideration four factors: the distance between the inlet and the floor (0.2–0.8 m), the depth of the cavity (2.5–17.5 cm), the intensity of solar radiation (400–1200 W/m^2), and the heating power of the fireplace (6.8–15.8 kW). Experimental results allowed for the determination of an SCH configuration. Other studies focused on developing solar chimneys for multi-zone buildings have been discussed in Refs. [48,49]. The described tests have been performed to enhance ventilation by adjusting the construction of the solar chimney.

In addition to the laboratory studies, some field tests have been conducted. Zha et al. [50] examined the operation of a solar chimney integrated with a building located in eastern China. The experimental results were compared with the outcome from numerical simulations. The authors noticed that for the solar chimney with dimensions 6.2 m × 2.8 m × 2.8 m and an air gap of 0.35 m, the airflow significantly varied during the daytime from 70.6 to 1887.6 m^3/h. Furthermore, the numerical simulation showed that during the transition

seasons, the energy-saving rate achieved using SCH was around 14.5% in Shanghai. Sivalakshmi et al. [51] conducted experimental research on ventilation by integrating a solar wall chimney in a room in India's warm climatic conditions. The wall's performance was examined for different air channel widths. Obtained results allowed us to summarize that the chimney's flow rate and air velocity rise with the widening of the air gap between the absorbing surface and the glass layer. The width of the air equal to 15 cm allowed us to obtain not only the highest air velocity (0.6 m/s) but also a maximum increase in air temperature (5.8 K). Frutos Dordelly et al. [52] experimentally tested the influence of integrating a PCM on the operation of two solar chimney prototypes built on a laboratory scale. The analyzed SCH was built with the usage of 2 cm plywood plates, characterized by a thermal conductivity of 0.15 W/(mK). The charge period with 550 W/m^2 irradiance was imitated by seven halogen lamps and lasted for 6 hours. It allowed for an average ventilation rate greater than 70 m^3/h. The obtained results allowed us to conclude that the integration of PCMs can increase the ventilation rate and provide a slower temperature drop during the discharge-only phase. Generally, implementing paraffin PCMs in SCHs may be considered an economically friendly solution for SCHs integrated with domestic buildings.

Among other numerical works, the authors in Ref. [53] prepared the theoretical models of the four solar chimney types working in heating or cooling mode. They aimed to estimate the air flow rate and temperature changes in the analyzed solar systems. Nguyen and Wells [54] created numerical models with the use of computational fluid dynamics (CFD) to examine the ventilation rate and the overall performance of SCHs integrated with building walls. Evaluated constructions included various chimney configurations, heat source locations, and four types of adjacent walls. Shaari et al. [55] presented the effect of a converging duct on the SCH using a CFD model in the ANSYS CFX software. The authors studied the effects of four configurations of bottom-to-top edge length ratio (1:1, 1:0.8, 1:0.75, and 1:0.5). Results showed that the 2:1 ratio allowed for the highest velocity at the outlet, whereas the 1:1 ratio provided the most efficient air exchange. Moosavi et al. highlighted the performance of an SCH combined with a windcatcher and water spraying system, which was dedicated to an office building. The obtained results of the experimental studies and CFD analysis highlighted that the SCH, integrated with a windcatcher and water spraying equipment, provides beneficial thermal conditions and a high level of ventilation comfort. During the summer peak, this arrangement reduced an average temperature of 5.2 K and minimized the energy consumption for cooling by 75% and for ventilation purposes by 90% [56]. In Ref. [57], the authors proposed to combine radiative cooling (RC) with the solar chimney. The hypothetical building has an SCH on the roof's south side and an RC system on the north side. The authors studied three variants of opening layouts using ANSYS Fluent 2021. The results indicated that the radiative cooling cavity has a beneficial impact on the ventilation and cooling performance of the SCH. The study presented in Ref. [58] examined the influence of a movable louver mounted at the outlet on the operation of a naturally ventilated wall. The authors took various solar conditions into consideration for regular and low-emissivity glass layers. A numerical simulation prepared with CFD methods was used to analyze the problem of combining solar irradiation and buoyant ventilation between two semi-transparent layers. This analysis showed that the upward-opening louvers could promote ventilation. In the case of the optimal angle (45°), the louver was able to promote the natural flow of air by 10–14%. On the contrary, the set-down louvers (angle between 112.5 and 150°) significantly reduced the natural flow by 6–9% for each 10°. He and Lv [59] used CFD simulations to examine the effect of the application of solar-absorbing plates on the building's ventilation. Firstly, experiments allowed us to observe that additional insertions enhanced the air flow by 1/3. Thus, absorbing plates were integrated with an SCH to distribute the heat more evenly. The results from CFD simulations allowed us to estimate that the analyzed method can enhance airflow by 57% compared to the basic configuration. Furthermore, Hweij et al. [60] investigated the operation parameters of a window in the office space cooled by evaporation with a 3-D CFD model. Two representative hours were selected for analysis, taking into consideration

the location of Riyadh (Saudi Arabia). This city is characterized by hot and dry climate conditions. The results allowed for a noticeable enhancement of thermal comfort in the office when the discussed system was operated. Taking into account a comfort scale from −4 (very uncomfortable) to +4 (very comfortable), thermal comfort reached a level of 1.42 at 14 h and 1.96 at 17 h. On the other hand, Selehi et al. [61] determined which periods of the year may be considered the most suitable for the use of an SCH in terms of thermal comfort. In order to study this problem, a dynamic thermal model of a residential building was prepared in EnergyPlus software. The authors took into consideration locations characterized by different hot climatic conditions: Bandar-Abbas (hot and humid) and Yazd (hot and arid). Obtained results from numerical simulations allowed us to state that the optimal time for operation of the SC for these cities is: November and January–April in the case of Bandar-Abbas, and April–May together with September–October for Yazd. These studies were continued by Nateghi and Jahangir [62]. The authors used EnergyPlus to simulate three house models: without a solar chimney, with SCH, and with SCH filled by PCMs. They focused on the thermal comfort provided by these variants of houses in three locations: Bandar Abbas (hot–humid), Yazd (hot–arid), and Tehran (cold–semi-arid). Obtained data highlighted that integration of PCM with an SCH leads to worsening thermal comfort in hot–arid climates. Nevertheless, PCMs positively influenced the SCH in terms of providing thermal comfort in all analyzed locations, regardless of the climatic zone. Furthermore, the study presented in Ref. [63] investigated the performance of a cooling system that combined evaporation's cooling effect with the buoyant flow in a solar chimney. A predictive numerical model of heat transport was prepared to analyze the behavior of this system in the case of its application in office space under the extremely hot climatic conditions of Riyadh, KSA. The results of this validated model showed that the proposed cooling installation is able to reduce the space load by almost 20%. Moreover, the interior, with a window-to-wall ratio of 40%, allowed for a more homogenous radiation distribution.

A brief summary of the main findings resulting from the discussed works is presented in Table 1.

Table 1. The summary of works focused on solar chimneys.

Authors	Parameters/Objective	The Main Findings	Conducted Works	Ref.
Villar-Ramos et al. (2020)	Study the energy performance of the single-channel SCH, considering the variation in energy absorbed by the absorber plate, the air gap, and the inclination angle	• SCH can work as a passive ventilation system; • Airflow can be enhanced up to 5 times, with a maximum efficiency of 88.9%.	Numerical study	[43]
Cheng et al. (2018)	Optimization of the SCH on both natural ventilation and smoke exhaustion with consideration of the height of the cavity inlet from the floor, cavity depth, solar radiation, and fire size	• An SCH configuration of 12.5 cm cavity depth and 0.5 m high air inlet was optimized; • External radiation enhances natural ventilation, whereas its influence on smoke exhaustion is limited.	Numerical and experimental study	[46]
Zhang et al. (2021)	Examine the airflow characteristics inside the SCH and the attached ventilated multiple zones, together with SCH performance, under various configurations and external environment	• The increase in the chimney height and location of the inlet enhances the airflow rate; • The non-optimal cavity gap and inlet size have minimal impact on the airflow rate; • The aspect ratio of the room shows a limited impact on the ventilation performance.	Numerical study	[47]
Sivalakshmi et al. (2021)	Analysis of room ventilation by integrating the SCH in the warm conditions of India	• The flow rate in the SCH increase with the increase of air channel breadth between the absorber and glass; • The air channel width equal to 15 cm provides the highest air velocity and a maximum temperature variation.	Experimental study	[51]

Table 1. *Cont.*

Authors	Parameters/Objective	The Main Findings	Conducted Works	Ref.
Frutos Dordelly et al. (2019)	Investigation of the impact of integrating PCMs on the performance of two prototypes of SCH	• PCMs integration provides a higher ventilation rate and a slower decrease during ventilation-only phases; • The implementation of paraffinic PCMs in SCH could be an economically viable option to create a healthy indoor environment within residential buildings through solar energy.	Experimental study	[52]
Nguyen and Wells (2020)	Prediction of the performance of the SCH with a horizontal air channel in terms of the induced air flowrate and thermal efficiency	• The flowrate increases with the length of the absorber surface, the gap of the air channel, and the heat flux; • As the outlet width increased, the flowrate increased until a critical value of the outlet width; • The outlet width significantly influences the thermal efficiency.	Numerical study	[54]
Moosavi et al. (2020)	Evaluate the cooling and ventilation potential of a solar chimney with and without the windcatcher functioning	• The SCH, with a windcatcher and water spraying system, provides good indoor conditions in terms of thermal and airflow even during hot and sunny periods; • The SCH with a windcatcher and water spray reduced an average temperature of 5.2 °C, as well as saved 75% of the cooling energy and 90% of the ventilation energy in the prototype building.	Numerical and experimental study	[56]
Suhendri et al. (2022)	Evaluation of the performance of the combined SCH and radiative cooling ventilation	• The combination of the SCH, radiative cooling, and wall-openings can preserve the ventilation performance even late at night until early morning; • The radiative cooling cavity can potentially be a passive precooling channel for the incoming fresh air; • Combining the radiative cooling cavity with the SCH can enhance the ventilation and cooling performance of conventional SCH ventilation.	Numerical study	[57]
HE and Lv (2022)	Examination of an innovative approach to enhancing the SCH effect of using solar energy for building ventilation	• Adding two solar absorbing plates increased the mass flow rate by 30; • The CFD simulations indicated that the insertion method could provide a 57% increase in flow rate over the base case without insertions.	Experimental and numerical study	[59]
Hweij et al. (2017)	Investigation of the evaporatively-cooled window driven by SCH integrated with façades for providing thermal comfort in an office space	• The proposed system improved occupant's thermal comfort at 14 h and 17 h in office space located in hot and dry climate conditions in Riyadh; • A noticeable reduction in energy consumption was obtained compared to a space providing approximately the same comfort level without the use of the proposed system.	Numerical study	[60]
Nateghi and Jahangir (2022)	Investigation of the influence of combining PCMs on SCH efficiency in three different climates	• PCMs could improve the performance of SCH when the temperature difference between night and day is high; • PCM was most effective in cold–semi-arid climates, especially during heating mode; • PCM can be tested in buildings with SCH and located in the semi-cold and dry climates.	Numerical study	[62]

3.2. The Classic Trombe Walls

The worldwide literature includes numerous studies focused on the improvements in the classical Trombe wall design. The possible improvement can be classified mainly into three aspects: air channel designs, material designs (including thermal insulation designs), and inlet and outlet air openings control.

The most efficient geometric configuration of a Trombe was numerically analyzed by Fidaros et al. [64]. The authors provided a 2D steady-state CFD model of a basic wall and validated it by comparison with the results of an energy balance model. Then, ten different

geometrical configurations were analyzed and compared. According to the results, the optimum width of the air gap varies between 5 and 8 cm. Moreover, the best configuration of the upper opening is an inclination of 30 degrees. Ref. [65] investigated the operation characteristics of the Trombe wall with a novel wavy shape. The experimental tests showed that this construction with an intersection angle of 90° or 120° could improve the overall performance. Especially the TW with an intersection angle of 90° is characterized by higher values of heat flux than the conventional flat wall. As was investigated, a wavy-shape TW with a properly adjusted intersection angle is characterized by better energy performance than a conventional TW. Owczarek [66] analyzed the heat transfer in a massive wall made of bricks operating under environmental conditions. The author collected data about temperature and solar radiation from several points located at the analyzed wall. The results showed a significant difference between operations in the winter and summer. During the summer, the difference in temperature between the external and internal surfaces of the wall reached the maximum value of 20 K, and the heat input was 80 W/m^2. During the winter, the greatest temperature difference decreased about two times, and the solar heat flux was lower than the measured energy loss through the wall. The author confirmed that the amount of heat collected and accumulated in the Trombe wall stabilizes after a few days of operation. Blotny and Mens [67] propose a passive TW system that may be used for both heating and cooling purposes. The installation was located on the southern wall of a building in Wroclaw, Poland. The authors provided numerical studies in the Ansys Fluent software to evaluate the distribution of temperature and the pattern of air circulation in the interior during the two-day-long operation. Obtained results showed a morning increase in temperature of 1.1 K and an afternoon decrease of about 2.3 K. Then, two variants of the TW were proposed: (I) the use of three-layered glazing with gaps filled with argon, and (II) the use of brick as the wall material instead of concrete. Zhu et al. [68] discussed the TW with an insulated panel located on its inner side. The bottom of the panel was accompanied only by the vents, whereas its upper edge had mechanically ventilated vents for stable air circulation control. The authors examined the thermal performance of this TW and concluded that the heat load was minimized by 27.3% compared to the classic TW and by 32.1% compared to the case without the TW. Applying two layers of glass instead of one saved 41.3% of the heat load. The authors in Ref. [69] presented a double-layer TW equipped with a fan. This system was installed in Kitakyushu, Japan, in an office building. The temperature of the ventilated air cavity of the TW and the indoor temperature were simulated using THERB for HAM software. The obtained data allowed us to conclude that the double-layer TW equipped with a DC fan to control the temperature limited the annual heating consumption by approx. 0.6 kWh/m^3 and simultaneously improved the wall performance by up to 5.6%. Lohmann and Santos [70] examined the thermal performance of the TW incorporated in a compartment located in Coimbra, Portugal. The authors compared two cubical modules made of lightweight steel that were exposed to environmental operating conditions. Results from these experiments allowed validation of the dynamic model of the analyzed system. According to the results, a TW significantly improved the module's thermal operation and reduced heat consumption. Nevertheless, to achieve these benefits, the system has to be well-designed for specified operating conditions and actively controlled to reduce the heat losses occurring during the night. Additionally, Miasik and Krason [71] studied the operation of a storage wall located on the southern side of a light-construction building. During the summer period, the roller shutters allowed reducing the heat flux by approx. 77% and therefore limited the building overheating. In the winter months, the level of energy consumption of the Trombe wall was comparable to that of a traditional wall (gains from solar radiation compensated for the lack of thermal insulation). The authors in Ref. [72] calculated the intensity of solar radiation reaching the outer surface of the Trombe wall in Harbin. This analysis included the impact of cloudiness. The results showed that the proposed Trombe wall leads to 61% annual savings in heat energy, whereas in the coldest month, these savings are only 32%. Kostikov et al. [73] determined that the most effective climate conditions for the operation of Trombe walls

are in locations with latitudes from 40 to 55. In these locations, the annual energy savings vary from 30 to 70%, leading to a payback time of 3.5–10 years, depending on the fuel cost. Another design of the modified Trombe wall was developed by Mohamad et al. [74] for heating and ventilating rooms during the winter period and for minimizing the need for cooling during the summer. The proposed installation utilized a container filled with water, traditionally used for the accumulation of hot water. The authors developed the mathematical model of the proposed system to determine the effects of various parameters on the effectiveness of heat transfer. In Ref. [75], the authors compared in terms of thermal performance three variants of buildings: (I) the conventional building characterized by lightweight construction, (II) a building equipped with the traditional Trombe wall, and (III) a building with a Trombe wall additionally integrated with PCMs. The dependence between the temperature of phase change in PCM and thermal comfort has been examined. It was concluded that during the summer period, the PCMs located next to the inner surface of the wall allowed regulation of the air temperature in the building more effectively than in the case of PCMs mounted closer to the outer wall surface. Therefore, the daily temperature profile was more uniform, preventing extreme peaks and overheating problems. During the winter months, the PCMs installed next to the inner surface enhanced heat transport to the building interior. Furthermore, a novel solar air heater has been developed and described in Ref. [76]. Two system configurations have been investigated: (I) a solar chimney and (II) a thermal storage wall. Both variants were first examined experimentally on the dedicated indoor stand. Collected data allowed the development of a numerical model in the ArCADia BIM software. The overall efficiency of the first construction (the solar chimney) was estimated at 0.25. The higher value, 0.78, was achieved in the case of the thermal wall. Both arrangements reduced energy consumption during the year by 191 kWh and 556 kWh, respectively (4.8 and 14.0%). As was concluded, these values can be greatly improved only by geometrical modifications such as increasing the overall length and modifying the shape of the studied accumulation heat exchanger.

Ozdenefe et al. [77] conducted a parametric study by varying the TW area from 6.0 m^2 to 16.2 m^2 to perform energy and economic assessments. As was shown, constructing a TW was economically viable for a thermally insulated building where the exemplary living room was only occupied in winter. If the building was not thermally insulated, constructing a TW was only feasible if its area was greater than 9 m^2. If the room was used in summer, there was an extra cooling load due to the existence of the TW, and economic feasibility was only achieved if there was insulation in the building. Bojić et al. [78] compared buildings' energy and environmental performance with and without Trombe walls. The investigations revealed that the building with TWs in Lyon, France, using solar energy can save around 20% of the operating energy during heating compared to that used by the building without TWs. For maximum primary energy savings and minimum benefit to the environment, the core layer in Trombe walls has to have the optimum thickness. In the case of electrical heating, the optimum thickness of the clay-brick core layer was estimated at around 0.35 m, and in the case of natural gas heating, it was calculated at around 0.25 m. Furthermore, Zhang and Shu [79] proposed a method to evaluate the energy, economic, and environmental performance of Trombe walls during a heating season. Firstly, non-iteration calculation methods were introduced for the energy evaluation of TW and conventional walls during the heating season. Then the economic and environmental evaluation models were brought out. Finally, a residential building was presented as the case building to evaluate TW's performance in five building climate zones in China. The calculation results showed that both heating degree days and solar radiation significantly impacted the energy-saving effect of Trombe walls. Stazi et al. [80] introduced an integrated approach for optimizing energy and environmental performances of complex building envelopes that combines life cycle assessment, energy simulation, and optimization analysis with the factorial plan technique. The environmental performance was calculated regarding energy demand and CO_2 emissions in the production and operational phases. Results of the optimization analysis demonstrated that it is possible to reduce the CO_2 emissions and

cumulative energy demand of solar walls for both the production and use phases by up to −55% compared with a traditional design.

A brief summary of the main findings resulting from the discussed works is presented in Table 2.

Table 2. The summary of works focused on the classic Trombe walls.

Authors	Parameters/Objective	The Main Findings	Conducted Works	Ref.
Fidaros et al. (2022)	Investigation of the optimal geometric configuration of a TW with a simulation of the transfer phenomena	• A 30 cm thick storage wall increases the air mass flow rate by 73% when compared to a wall with a thickness of 15 cm; • When high air exit temperatures are required, a small gap width of 5 cm is suggested, and when high room-facing storage wall surface temperatures are required, a gap width of 7–8 cm is suggested.	Numerical study (2D steady-state CFD model)	[64]
Chem et al. (2022)	Study of the energy performance of the novel TW characterized by the wavy shape	• The stainless steel painted with black solar-absorber paint reached the highest average surface temperature and took the least time in the heating procedure; • The 90° and 120° intersection angle models have better performances than the flat model in all aspects of air velocity, surface, and airflow temperatures; • A wavy-shape TW with a proper intersection angle has a better energy performance than a traditional TW during a considerable period of daytime.	Numerical study	[65]
Zhu et al. (2022)	Study of a new composite TW with an additional layer of thermal insulation which created two air layers	• A composite TW equipped with a temperature-controlled DC fan leads to higher energy savings than a classic TW; • Compared to single-glazing, double-glazing allows for saving 41.3% of the primary energy consumption; • The thickness of the massive wall directly affects its thermal operation; • Higher ventilation volume allows for storage of a higher heat load, but only for specified ventilation ratios.	Numerical study	[68]
Lohmann and Santos (2020)	Evaluation of the influence of a passive water TW on the thermal behavior and energy efficiency of a lightweight steel frame compartment	• TW was more suitable for an office application (only during the daytime), instead for a residential building; • An increase in the original TW air cavity thickness (10 cm) and the wall thickness (5 cm) does not affect thermal performance.	Numerical study	[70]
Miąsik and Krasoń (2021)	Study of the possibility of using a mass collector-storage wall integrated into the structure of a building with a light skeleton structure	• The use of a TW in the southern facades of frame-based buildings is justified; • The effect of using the roller shutters is a reduction in the average heat flux value by approx. 77%; • The high storage of the wall has a positive effect on the air temperature in the room by making it more stable.	Numerical and experimental study	[71]
Kostikov et al. (2020)	The calculation for forecasting solar radiation intensity on a Trombe wall surface	• In the case of Harbin climatic conditions, a TW can allow providing 32% of the required amount of heat energy in the coldest month; • Annual savings in heat energy resulting from the implementation of the TW are approx. 61%; • The TW, as an additional heat source, is a reasonable option for the heat supply system in the set climatic conditions.	Numerical study	[72]
Kostikov et al. (2020)	Determination of the most effective climate divide for the TW	• The most appropriate TW use in the heat supply system is observed in the range of latitudes from 55° to 40° N; • The payback period of the TW is in the range of 3.5 to 10 years.	Numerical study	[73]
Li et al. (2022)	Comparison of the thermal performance of a traditional lightweight building, traditional TW building, and TW building with PCMs	• In summer, compared with the PCM installation next to the outer surface, the PCM next to the inner surface regulated the indoor air temperature more effectively, which reduced the indoor air peak temperature and prevented overheating problems; • In winter, the PCM next to the inner surface improved the air temperature in the air channel, and more heat was released indoors compared with the PCM installation next to the outer surface; • In the region with hot summer and cold winter climates, priority should be given to the TW system with PCM25 placed next to the inner surface.	Numerical and experimental study	[75]

Table 2. *Cont.*

Authors	Parameters/Objective	The Main Findings	Conducted Works	Ref.
Sornek and Papis-Frączek (2022)	Development of a novel configuration of the solar air heater composed of inexpensive accumulative material	• Solar radiation heats the ceramic material, and collected energy may be used to preheat the inflowing air; • The total efficiency of the ceramic solar chimney was estimated as 0.25; • The total efficiency of the ceramic thermal wall was estimated at 0.78.	Numerical and experimental study	[76]

3.3. Trombe Walls with Incorporated Phase Change Materials

The installation of the PCMs is an appealing option from the standpoint of improving the energy efficiency of the buildings. Phase change materials are capable of storing and releasing the latent heat with minimal or almost no change in their temperature.

Among other investigations presented in the newest worldwide literature, Rehman et al. [81] proposed a novel configuration of a Trombe wall made of brick equipped with two layers of PCM. The wall was designed to maintain thermal comfort in climatic conditions in Islamabad, Pakistan. The authors provided a numerical simulation of the charging and discharging cycles of PCMs for two months: June and January. Results showed that the melting fraction for two layers of PCMs was 71% and 2% in June, whereas in January it was 58% and 100%. The continuous process of charging–discharging is essential for the high performance of the TW. The thermal performance of a brick wall with incorporated low-cost PCMs ($CaCl_2 \cdot 6H_2O$) and local organic waste materials (corn husk) has been numerically investigated in Ref. [82]. The work aimed to reduce energy usage in low-cost buildings. The analysis of temperature distribution allowed the maintenance of a maximum interior temperature of 27 °C, compared to 31 °C in a house with traditional brick construction, which proved the legitimacy of Trombe walls enhanced with PCMs and biomass waste. Furthermore, Leang et al. [83] demonstrated the influence of PCMs on the thermal performance of the storage wall. The authors investigated three dynamic models: (I) a traditional house without any solar systems, (II) a house with a solar wall made of concrete, and (III) a house with a PCM solar wall. These cases were studied under three different climate conditions. Obtained data showed that Trombe walls minimized the heating demand by about 20% compared to the reference house. Moreover, the authors highlighted that a solar wall of any kind is not able to satisfy the total heating demand but should be used as an additional source of clean energy. Lichołai et al. [84] determined the impact of glazing on the thermal performance of the TW with PCM. Experimental studies included three variants of glazing with varying heat transfer coefficients and transmittance factors. Laboratory studies were carried out in a small-scale simulation chamber. A significant impact of the glazing type on the performance of TW was found. The obtained numerical results showed good consistency with those of the experimental studies. In Ref. [85], the authors provided a comparative energy analysis for a traditional building equipped with a TW and a building with both a TW and a PCM. Results showed that the TW located on the southern building façade significantly increased the indoor air temperature and, therefore, reduced the annual heat demand from 4 185 to 3 075 kWh. On the other hand, the TW in the summer showed a negative impact on the building's energy balance—the interior temperature was too high to maintain thermal comfort, so air cooling was necessary. In the building equipped with the PCM Trombe wall, energy demand was reduced in the winter and summer. As was investigated, during periods without enough solar energy, the heat accumulated in PCMs may enhance air circulation and therefore reduce the energy demand by almost 20%. During hot periods, PCMs successfully prevent interior overheating. Tempierik et al. [32] numerically studied the PCMs' melting process to prevent their overheating in Trombe walls. The simulations showed that the top part of PCM heats up faster than the lower part, which can lead to a significant temperature gradient alongside the TW. To solve this problem, authors proposed dividing PCMs into smaller parts with smaller volumes each or using in one wall different types of PCMs, which show a difference in melting temperatures. Another example of

comparative research on the characteristics of buildings without TW, with conventional TW, and with TW with additional insertions has been presented in Ref. [86]. The authors provided simulations using Autodesk® CFD software. These simulations have proceeded with three flats characterized by an area of 55 m^2, 75 m^2, and 95 m^2. Each case was analyzed for six months. As was observed, the thermal comfort in the conventional building was relatively low, with an average score of −1.86. In the case of TW, with the insertion of the porous medium, it was better, reaching an average level of +0.10. In Ref. [87], calculations based on machine learning have been applied to forecast the thermal performance and the pattern of air flowing through porous media in TWs. The authors prepared a CFD calculation of the analyzed wall over a 24-h period. To simulate the solar conditions, the Monte Carlo radiation model was activated. The prepared model allowed us to predict and optimize the concentration of PCM in the TW construction. It was calculated that PCMs could reduce the temperature of porous walls by 5.2% and decrease the temperature gradient by about 6.3% compared to the conventional TW. Furthermore, Simões et al. [88] assessed the impact of the TWs integrated with the building on the building's energy performance in the Mediterranean climate. Shading devices, including overhangs and blinds, were mounted on the air vents. The performance of the proposed system was simulated using EnergyPlus and DesignBuilder software. The results demonstrated that TWs equipped with shading devices could significantly reduce energy demand if they were adjusted to the specific daily and seasonal operation needs. The proposed TW system reduced the demand for heating power by approx. 20%. Authors have also observed that active ventilation during the night may limit the cooling demands by approx. 35%. Mabrouki et al. [89] discussed TW's operational aspects in Morocco's semi-oceanic climate. The authors searched for the optimal parameters of the TW used in a semi-oceanic climate. The highest reduction in primary energy consumption was found for an air gap of 3 cm, a sunshade of 0.9 m, and RT 28 HC as PCM. Under these conditions, the energy demand for the reference house decreased by 42.97% (from 1286 kWh/a to 733 kWh/a). The dynamic model of the heat transfer between TW with PCM and an exemplary room was presented by Zhu et al. [90]. The authors combined the heat transfer model prepared in TRNSYS with the GenOpt optimization tool. This allowed for estimating the system's energy demand and analyzing the influence of six selected factors on the overall performance. These "essential influencing" factors were: the thickness of an air gap, external sun-shading, the total thickness of TW, presence of vents, and the thermal properties of PCMs used in the upper and lower layers of TW. The annual energy consumption was reduced by 7.56% using optimized TW instead of traditional TW. To assess the efficiency of wall-integrated PCMs, five variants of solar walls have been simulated by Fateh et al. [91]. Each wall was characterized by a different location of PCMs. The results showed that PCMs are more effective when temperature changes are similar to their phase change temperature. As was observed, the additional layers of PCMs may reduce the energy consumption by approx. 75%. Finally, the authors summarized that the effectiveness of PCMs application strongly depends on the complex combination of coupled effects [85]. Furthermore, Tlili et al. [92] transiently simulated a room with a Trombe wall using COMSOL software. The authors analyzed two configurations of the wall. Each consisted of four blocks of PCM and four cement bricks of the same size. The freezing time of PCM has been studied under various sizes of the air inlet and outlet (10–30 cm). Moreover, this study included an interior temperature and air velocity analysis in relation to the temperature and the fraction of PCMs. Obtained results allowed for concluding that the use of PCM prolongs the duration of natural air circulation by up to 12 h. Generally, the indoor air velocity increased and the outlet temperature decreased with the widening of the inlet. The authors in Ref. [93] investigated the performance of PCM walls for solar space heating. The PCM walls consisted of brick walls, plasterboards containing PCMs, and novel triple-glazing units. The overall efficiency of the PCM walls was experimentally determined on a monthly basis. In addition to the experimental analysis, a theoretical energy analysis of the PCM walls based on 10-year mean meteorological data was performed. Theoretical analysis

showed that the reduction of CO_2 emissions on a monthly basis varied from 57 to 7% during the heating period. The reduction of CO_2 emissions was 16% on an annual basis.

Furthermore, Zhu et al. [94] summarized recent research progress on several categories of functional coatings, emphasizing their applications for green and intelligent buildings. These included hydrophobic coatings, hydrophilic and photocatalytic coatings, and PCM coatings. The authors aimed to provide a general introduction and research progress on these selected functional coating technologies, from the material's fabrication to its application in different building components. Soo et al. [95] reported a new type of solid-solid PCM based on chemically linked polyethylene glycol with polylactic acid as a block co-polymer. As was explained, in contrast to solid-liquid PCMs (which are exposed to leakage and leaching), solid-solid PCMs can overcome these issues due to their inherent form stability and homogeneity. Solid-solid latent heat of up to 56 J/g could be achieved, with melting points between 44 °C and 55 °C.

A brief summary of the main findings resulting from the discussed works is presented in Table 3.

Table 3. The summary of works focused on the Trombe walls with incorporated PCMs.

Authors	Parameters/Objective	The Main Findings	Conducted Works	Ref.
Rehman et al. (2021)	Investigations of the effectiveness of dual PCM application to increase the thermal mass of construction materials	• Dual PCM configuration is beneficial for both summer and winter periods; • The continuous process of charging-discharging is highlighted as the main advantage of the dual PCM system; • Average indoor temperatures with and without PCMs for June are 21.6 °C and 35 °C, while for January are 20.7 °C and 12.1 °C, respectively.	Numerical study	[81]
Rehman et al. (2021)	Investigation of the thermal response of a hybrid building envelope, including PCM and local organic waste materials	• Sustainable and organic waste materials such as corn husks, rice husks, and wheat straw used in construction materials can save energy demand; • The combination of PCM and the corn husk stabilizes the indoor temperature and provides thermal comfort for inhabitants; • Composite blocks are considered suitable construction materials for low-cost buildings.	Numerical study	[82]
Leang et al. (2020)	Demonstration of the impact of PCMs integrated into the storage wall on the thermal energy performance of TW	• The installation of a TW, regardless of the configuration, allows to reduce the room heating energy demands by about 20–30% (depending on the climatic conditions); • PCM integrated with mortar has a weak effect on energy demands (about 2% compared to mortar alone).	Numerical study	[83]
Yang et al. (2022)	Investigation of the primary energy usage in the building with the installed TW	• The TW had an acceptable performance in reducing the primary energy usage by 26.5% in winter while increasing the primary energy usage by 5.5% during the year; • By adding PCM to the TW, the primary energy usage in all months decreased, and in one year, the primary energy usage decreased by 18%.	Numerical study	[85]
Facelli Sanchez et al. (2022)	Analysis of the performance of dwellings without TW, with traditional TW, and with TW with glass and plastic pellets insertion in thermal comfort improvement	• The performance of TW with acrylic pellets insertion increases the internal temperature by up to 155% compared to a traditional system without TW; • The TW with Acrylic Pellets insertion system outperforms the TW with Glass Pellets insertion and the classic TW in increasing the temperature and thermal comfort in residential buildings.	Numerical study	[86]
Saboori et al. (2022)	Simulation of the flow pattern and the thermal behavior through pore scale porous media walls, including PCMs in TWs	• PCMs can reduce the temperature of pore scale porous media wall (outer side) by 5.2% compared to the without PCM state over day and night; • The temperature gradient over the day was 6.34% lower than it was when PCMs were not used; • For the period from 17:00 to 06:00, the average temperature of the pore scale porous media wall with PCMs was up to 6.64% higher than it was without PCMs.	Numerical study	[87]

Table 3. *Cont.*

Authors	Parameters/Objective	The Main Findings	Conducted Works	Ref.
Simões et al. (2021)	Assessment of how subtypes of the Mediterranean climate would affect the energy performance of TWs integrated with building envelope	• TWs can lead to significant reductions in energy consumption if properly tailored shading devices and vents with specific daily and seasonal operation schedules are implemented; • The TW system helped to cut demand for heating by approx. 20%; • In the southernmost locations, the inclusion of night ventilation led to a decrease in cooling demands by approx. 35%.	Numerical study	[88]
Zhu et al. (2021)	Analysis of the six key influencing factors affecting the thermal and energy performance of PCM Trombe wall system, including thermal storage wall thickness, air gap thickness, vents area, external sun shading length, melting temperature of lower temperature PCM layer, and higher temperature PCM layer	• After adding PCM layers to the traditional TW system, the optimal values of air gap thickness, vents area, and thermal storage wall thickness were not changed; • Compared with the optimized traditional Trombe room, the annual total building load was reduced by 7.56% and 13.52% in the optimized reference Trombe room and optimized PCM Trombe, respectively; • The energy-saving effect in the PCM Trombe room was better than that in the reference Trombe room compared with the traditional Trombe room.	Numerical study	[90]
Tlili and Alharbi (2022)	Evaluation of heat consumption due to heat transfer through the South, East, West, and North facing a plane wall with insulation in the form of PCMs	• Insulation layers with PCMs could lead to energy savings of up to 75% of the heat load through opaque walls; • PCMs inside the northward-facing wall do not generate a sensible reduction of energy consumption and, in most conditions, they even increase heat transfer through the wall; • Using PCMs has a strong effect on the reduction of the energy consumption for the side walls, even higher than for the South facing wall.	Numerical study	[92]

3.4. The Photovoltaic Trombe Walls

The integration of PV cells with the TWs is effective in the case of thermal regulation of buildings and electrical energy production. Authors in Ref. [96] examined the built-middle PV Trombe wall (PVMTW), characterized by the PV cells' presence in the middle of the air gap. Its performance was compared with the traditional built-external PV Trombe wall (PVGTW) under the conditions of Hefei, China. The obtained results showed that the average thermal and electrical performance of the PVMTW system was 38% and 12%, respectively, whereas the average total efficiency was about 11% higher than for the PVGTW system. This numerical model was first validated and then used to estimate the effects of channel length, the PV cells' position, and the PV cells' coverage ratio on the PVMTW energy performance. Obtained results showed that the modifications of these parameters do not affect electricity production but significantly influence its thermal performance. The authors determined that the optimal distance between the PV panel and the glass layer is between 12 mm and 30 mm. Due to this, the highest values of total, thermal, and electricity efficiency were obtained: 57.3%, 38.3%, and 12.0%, respectively. The design, construction, and performance of a PV blind-integrated TW are described in Ref. [97]. The authors conducted experimental measurements to analyze the effect of inlet airflow rates and PV blind angles on electrical and thermal gains. The most beneficial operating parameters were obtained under an angle of 50° and an airflow rate of 0.45 m/s. Then, the electrical performance of the PV panel was compared to the photovoltaic cells fixed on the exterior glazing and attached to the brick wall. Results showed that the highest electricity generation was obtained in the case of the PV panel located on the glass, whereas the two other variants gave similar results. The PV blind-integrated TW achieved the best total efficiency when considering heat gains and electricity generation. The study reported in Ref. [98] shows a PV blind-integrated TW system (BIPVBTW) under Hefei weather conditions. The authors investigated the optimal PV blind slat angles for three periods of the year: winter, summer, and mid-term season and time of day: 9:00–17:00. Obtained results highlighted that the annual electricity gain from the BIPVBTW system is on a similar level as in the BIPVGTW system, but about 20% higher than in the BIPVMTW system. The cooling load reduction is the highest in the case of BIPVGTW systems. When considering cooling and heating

load reduction and electricity generation simultaneously, the total savings of the analyzed BIPVBTW system are approx. 45% higher than in BIPVMTW/BIPVGTW installations.

In Ref. [99], the authors provided experimental and numerical studies to compare a conventional Trombe wall with one enhanced in the Venetian blind (TW_Ven). The experiments were carried out under the climatic conditions of Abha, Saudi Arabia. The numerical results were validated by comparison with the outcome from experimental tests. Obtained data indicated that the photovoltaic Thombe wall system with a Venetian blind (PVTW_Ven) with the slats at 60° can regulate the airflow and provide proper interior shading. The TW_Ven was characterized by 1.33 times more heat gains compared to the PVTW_Ven one. On the other hand, the maximum value of the temperature of the Venetian blind measured in the PVTW_Ven was lower by 4.7 K compared to the temperature observed in the TW_Ven. Furthermore, the thermal and electrical performance of a PVTW_Ven in semi-arid climatic conditions was investigated by Irshad et al. [100]. A 3D CFD model was developed. As was investigated, the optimal Venetian blind spacing within the air gap should be 0.09 m^2, the Venetian blind angle should be 60°, and the PVTW airflow rate should be at a level of 0.2 m/s. Moreover, PVTW-Ven was compared to the PVTW without the Venetian blind. The PV panel surface's average electricity production and temperature were 8.6% higher and 3.2 K lower in the case of the PVTW-Ven configuration, respectively.

Bruno et al. [101] used transient simulations in the TRNSYS software to assess the performance of PVTW. The empirical method based on solar load ratio (SLR) was calibrated by multiple linear regression to calculate the monthly demand for auxiliary energy in buildings. The proposed methodology confirmed its validity with average errors below 1.4%. Moreover, numerical results showed that thin-film PV cells do not influence the storage properties of the massive wall [92]. In Ref. [102], a bifacial photovoltaic module was combined with the building wall to create a bifacial PV wall (BI-PVW) system. An experimental rig was developed, and an analysis of energy utilization under various ventilation strategies was conducted. The efficiency of utilization of solar energy can reach approx. 40% on sunny days. Then, an analysis of the building with the BI-PVW system was carried out. As was calculated, ventilation can provide a 21.2% energy-saving effect on the building. Abed et al. [103] demonstrated the impact of a glass cover on the performance of the PVTW where nano-fluid in the form of water/Al_2O_3 was used as a coolant. Two concentrations of nanoparticles were tested (0.5% and 1.0%). The highest thermal efficiency was 80% (at 2 p.m., when using a glass cover and 0.5% nano-fluid), while the maximum level of electrical efficiency was 14% (at 1 p.m.). Finally, it was concluded that low-concentration nanoparticles with cooling water could improve the system's efficiency. The objective of the investigation presented in Ref. [104] was to study the impact of PV cooling on the overall performance of the PVTW system. To do so, the authors constructed two experimental stands. Results showed that the system with water cooling had the highest daily thermal efficiency (about 40%). On the contrary, the highest electrical efficiency (12%) was observed in the system with combined air-water cooling. Nevertheless, the best overall efficiency was found in the case of the water-cooled system (51%). Furthermore, Luo et al. [105] proposed a building-integrated photovoltaic thermoelectric (BIPVTE) wall. The authors numerically investigated its thermal and electrical performance and compared obtained results with a conventional concrete wall. The operation of BIPVTE was analyzed for Hong Kong and six other cities with similar climatic conditions. Obtained results indicated that the BIPVTE installation leads to energy savings at a level of 29.19–62.94 kWh/(m^2a), depending on the location [96]. Abdullah et al. [106] designed and utilized an empirical system to analyze the impact of PCM, DC fan, and heat exchange on a PVTW system. As was observed, the PCMs and the heat exchanger caused thermal and electrical efficiency values to rise by 1.5% and 3.0%, respectively. The DC fan and the heat exchanger increased electrical efficiency by 1.0% and thermal efficiency by 26.0%. Yu et al. [107] proposed a purified PVTW that allowed for producing sustainable electricity, degrading gaseous formaldehyde in a year, and realizing space heating and supplying hot water. As observed during the studies conducted

by 6 continuous full days, the average daily electrical and thermal air efficiency was at 11.9% and 36.6%, respectively. The clean air delivery rate ranged from 42.5 to 81.6 m^3/h, while the daily produced clean air volume was determined as 202.9 $m^3/(m^2 \cdot day)$. The thermal efficiency and electrical efficiency considering formaldehyde degradation was approx. 50.3%, with an increase of approx. 3.7% due to the contribution of formaldehyde degradation. A novel passive solar wall in the form of a photocatalytic-photovoltaic-Trombe wall (PC-PVTW), which could provide heat, electricity, and fresh air simultaneously, was discussed by Wu et al. [108]. The authors established a multi-physical field (temperature, velocity, and concentration) coupling model to analyze the performance of the proposed PC-PVTW system. The results showed that the ventilation volume, heat output, thermal efficiency, electrical efficiency, and clean air delivery rate of the PC-PVTW system presented different trends of decrease or increase with the variation of channel dimensions. As opposed to the effect on electrical efficiency, the lower ambient temperature negatively influenced the thermal performance, ventilation volume, and air purification performance, especially when lower solar radiation intensity was considered. As was concluded, the PC-PVTW system can utilize air purification, electricity generation, heating, and ventilation of solar energy. The total value of efficiency can reach a maximum level of 0.67.

A brief summary of the main findings resulting from the discussed works is presented in Table 4.

Table 4. The summary of works focused on the photovoltaic Trombe walls.

Authors	Parameters/Objective	The Main Findings	Conducted Works	Ref.
Lin et al. (2019)	Investigation of the impact of inlet airflow rates and PV blind angles on heat gains and electricity generation of the PVTW system	• The more significant the inlet air flow rate, the lower the PV cells' temperature and the temperature of the air at the outlet; • To balance the achieved benefits (space heating and electricity generation), the optimal inlet airflow rate was 0.45 m/s; • The highest electricity generation was observed in the PVGTW system, whereas the highest heat gains were noted in the case of the PVBTW configuration.	Experimental study	[96]
Islam et al. (2020)	Investigation of a novel configuration of a PVTW_Ven system installed in the air gap between the photovoltaic panel and the TW	• The outer wall and inner wall temperature of the PVTW_Ven was 5.2 °C and 3.6 °C lower, respectively, than those of the TW_Ven; • The average heat gains of PVTW_Ven were 33.5% lower than that of the TW_Ven; • PVTW_Ven system was preferred over the TW_Ven system because of the additional electrical energy generation and maintaining the required indoor temperature at the night.	Numerical study	[99]
Irshad et al. (2022)	Investigation of the thermal and electrical performance of a PVTW_Ven in semi-arid climatic conditions	• The proposed configuration of the PVTW_Ven reduced the indoor, wall, and PV cell temperatures compared to the standard PVTW; • The optimal configuration of the PVTW_Ven system had 45-mm blind spacing, 0.2-m/s airflow rate, and 60° Venetian blinds angles; • By the integration of Venetian blinds with the PVTW system, the maximum power generation from the PV panels was increased by 8.6%.	Numerical and experimental study	[100]
Zhao et al. (2022)	Study of the performance improvement of the system with a bifacial PV module combined with the wall	• By implementing the bifacial PV panel under the transparent glass, the improvement of comprehensive solar energy utilization can be achieved; • The increase in power generated in the bifacial PV wall compared to the mono-facial PV system was approx. 16% in winter and 19% in summer; • The comprehensive solar energy utilization efficiency can reach a level of 40% when the system is ventilated in an indoor environment in winter.	Numerical and experimental study	[102]

Table 4. *Cont.*

Authors	Parameters/Objective	The Main Findings	Conducted Works	Ref.
Abed et al. (2021)	Demonstration of the effect of a glass cover on the efficiency of the PVTW by the usage of nano-fluid as a coolant	• A low concentration of nanoparticles improves the effectiveness of the PVTW; • Placing the glass cover on the front of the TW causes an increase in the PV cell temperature, which decreases the electrical efficiency and increases the internal room temperature; • The highest recorded thermal efficiency at a level of 80% was observed at 2 p.m. when a glass cover and 0.5% nano-fluid were used.	Experimental study	[103]
Abdullah et al. (2022)	Study of the impact of the cooling method of the photovoltaic module on the PVTW system performance	• The implementation of a DC fan to the PVTW increases its performance by increasing heat gain and lowering PV panel temperature; • Water cooling of the PV panel allows for lowering its temperature and increasing the amount of energy produced; • Cooling the PV panel by placing a heat exchanger behind the PV panel in the PVTW system was more effective than other systems.	Experimental study	[104]
Abdullah et a. (2021)	Analysis of the impact of PCM, DC fan, and heat exchange on a PVTW system	• Using PVTW integrated with PCMs, DC fan, and heat exchange led to a lower PV cell temperature and improved room comfort; • The PCM and the heat exchanger caused thermal and electrical efficiency values to rise by 1.5% and 3.0%, respectively; • The combined influence of the heat exchanger and the DC fan increased electrical efficiency by 1.0% and thermal efficiency by 26.0%.	Experimental study	[106]
Yu et al. (2019)	Investigation of the comprehensive performance of novel solar thermal-catalytic photovoltaic and thermal recovery TW system	• The daily air thermal efficiency and average electrical efficiency of the purified PVTW were 36.6% and 11.9%, respectively; • The electrical efficiency to the cell standard efficiency ratio approached up to 98.6%; • The thermal and electrical efficiency considering formaldehyde degradation was at a level of 50.3%, with an increase of 3.7% due to the contribution from formaldehyde degradation.	Numerical and experimental study	[107]
Wu et al. (2019)		• With the increase of channel height, the airflow, heat output, thermal efficiency, electrical efficiency, and clean air delivery rate of PC-PVTW increase; • The variations in channel width affect the velocity field or flow state of air, which affects the PC-PVTW performance; • The lower ambient temperature has a negative impact on the airflow, thermal performance, and air purification performance when lower solar radiation intensity occurs.	Numerical study	[108]

4. Conclusions

There are various passive solar systems. Among them, the most popular are direct gain walls and thermal storage walls (known as Trombe walls). In the last decade, numerous studies dedicated to the Trombe wall systems were published, meaning there is a growing interest in this subject. This paper comprehensively reviewed the experimental and numerical studies devoted to the different solutions of Trombe walls, including solar chimneys, classic Trombe walls, Trombe walls with incorporated phase change materials, or photovoltaic cells.

The solar chimney is a passive ventilation system that uses buoyancy principles. Mathematical models of heating and cooling processes have widely described this technology. Moreover, the dependence between the operational parameters (solar radiation intensity, air flow, and wind interference) and construction of solar chimneys (size and configuration of the solar chimney, material properties, size of an air gap, and inclination angle) has been studied experimentally and numerically. Generally, the mass flow rate increases sharply while increasing the chimney gap. Moreover, the most convenient and effective way to improve solar chimneys' thermal performance is to change the system's configuration or

use more effective materials. Studies showed that optimizing chimney height and moving the air gap upward increased ventilation capacity by about 90%. Integrating PCMs, especially under hot–humid and cold–semi-arid climatic conditions, can also obtain a higher ventilation rate. Moreover, solar chimneys may be coupled with fireplaces, windcatchers, or water spray systems to save the energy required for ventilation.

The classic Trombe wall is made of massive heat storage materials such as brick, concrete, or stone and an additional layer (or layers) of glass. Available studies are focused on three aspects: air channel designs, material designs, and inlet and outlet air openings control. Generally, the optimum width of an air gap varies between 5 and 8 cm, whereas the best inclination of the upper ventilation slot is 30 degrees. An innovative way to improve the overall efficiency of a Trombe wall is to design it as a wavy shape to absorb more solar radiation. Experimental studies highlighted a significant difference between the operation of the Trombe wall in winter and summer, but in both cases, the amount of stored energy stabilizes after a few days. In unfavorable winter conditions, the gain from solar heat flux may be even lower than the energy loss through the wall. Nevertheless, using glazing and a temperature-controlled DC fan saves a significant amount of energy. During the summer months, the roller shutters reduce the building's overheating problem. Generally, the annual energy savings from using Trombe walls vary from 30 to 70%, depending mainly on the wall's configuration and climatic conditions.

To increase the thermal efficiency of the classic Trombe wall and reduce the temperature fluctuations on its surface, the wall can be filled by latent storage materials (PCMs). Some studies included incorporating local organic waste materials or porous medium alongside the PCMs. The key factors influencing the thermal performance of Trombe walls with PCMs are the number and thickness of air gaps, the construction of wall layers, and the melting temperatures of used PCMs. Generally, the lowest risk of overheating in summer is noted for ventilated walls made of massive materials such as bricks. Furthermore, the application of glazing has a noticeable influence on thermal operation. To avoid problems with the non-homogenous melting of PCMs, which can lead to a significant temperature gradient along the wall, a large volume of PCMs should be divided into smaller parts.

Another upgrade of the classic Trombe wall includes PV cells, which generate electricity. The influence of channel height, the PV cells' coverage ratio, and their position significantly impact thermal performance, whereas they have little effect on electrical efficiency. Thin-film PV cells do not influence the storage properties of the massive wall. Higher electricity generation is obtained in the case of a PV panel located on the outer glass layer than in the case of a panel mounted on the brick wall. Moreover, the introduction of an air- or water-cooling system allows for to reduction of the negative temperature effect on the PV cells' efficiency. The application of blinds allows for regulating the airflow and provides proper interior shading. Novel multi-functional passive photovoltaic solar walls are constantly developed. Systems such as photocatalytic-photovoltaic-Trombe wall (PC-PVTW) or photovoltaic thermoelectric (BIPVTE) walls give promising results, but further investigation is needed.

The majority of analyzed studies showed that the application of these systems in residential and non-residential buildings usually leads to energy savings, lower emissions of greenhouse gases, and improvement of both thermal comfort and living standards. The actual state of the art is presented in the context of reducing energy consumption and enhancing thermal comfort. However, there is a need for more detailed feasibility studies, including cost and environmental indicators.

Funding: This work was carried out under Subvention no. 16.16.210.476 from the Faculty of Energy and Fuels, AGH University of Science and Technology in Krakow. This research project was partly supported by the program "Excellence initiative—research university" for the AGH University of Science and Technology.

Data Availability Statement: Not applicable.

Conflicts of Interest: The authors declare no conflict of interest.

References

1. Santamouris, M.; Vasilakopoulou, K. Present and future energy consumption of buildings: Challenges and opportunities towards decarbonisation. *e-Prime-Adv. Electr. Eng. Electron. Energy* **2021**, *1*, 100002. [CrossRef]
2. Krawczyk, D.A. Analysis of Energy Consumption for Heating in a Residential House in Poland. *Energy Procedia* **2016**, *95*, 216–222. [CrossRef]
3. Filippidou, F.; Nieboer, N.; Visscher, H. Are we moving fast enough? The energy renovation rate of the Dutch non-profit housing using the national energy labelling database. *Energy Policy* **2017**, *109*, 488–498. [CrossRef]
4. Li, Y.; Li, M.; Sang, P.; Chen, P.-H.; Li, C. Stakeholder studies of green buildings: A literature review. *J. Build. Eng.* **2022**, *54*, 104667. [CrossRef]
5. Xiang, Y.; Chen, Y.; Xu, J.; Chen, Z. Research on sustainability evaluation of green building engineering based on artificial intelligence and energy consumption. *Energy Rep.* **2022**, *8*, 11378–11391. [CrossRef]
6. Entrop, A.G.; Brouwers, H.J.H. Assessing the sustainability of buildings using a framework of triad approaches. *J. Build. Apprais.* **2010**, *5*, 293–310. [CrossRef]
7. Alavirad, S.; Mohammadi, S.; Hoes, P.-J.; Xu, L.; Hensen, J.L. Future-Proof Energy-Retrofit strategy for an existing Dutch neighbourhood. *Energy Build.* **2022**, *260*, 111914. [CrossRef]
8. Shayan, M.E. Solar Energy and Its Purpose in Net-Zero Energy Building. In *Zero-Energy Buildings—New Approaches and Technologies*; IntechOpen: London, UK, 2020. [CrossRef]
9. Żołądek, M.; Filipowicz, M.; Sornek, K.; Figaj, R.D. Energy performance of the photovoltaic system in urban area-case study. In *IOP Conference Series: Earth and Environmental Science*; IOP Publishing: Bristol, UK, 2019; Volume 214, p. 012123. [CrossRef]
10. Goel, V.; Hans, V.; Singh, S.; Kumar, R.; Pathak, S.K.; Singla, M.; Bhattacharyya, S.; Almatrafi, E.; Gill, R.; Saini, R. A comprehensive study on the progressive development and applications of solar air heaters. *Sol. Energy* **2021**, *229*, 112–147. [CrossRef]
11. Olczak, P. The comparison of solar installation heat gains and SHW simulation results—Case study. *Polityka Energetyczna—Energy Policy J.* **2020**, *23*, 41–54. [CrossRef]
12. Peters, I.M.; Hauch, J.A.; Brabec, C.J. The role of innovation for economy and sustainability of photovoltaic modules. *IScience* **2022**, *25*, 105208. [CrossRef]
13. Calise, F.; Figaj, R.D.; Vanoli, L. Experimental and Numerical Analyses of a Flat Plate Photovoltaic/Thermal Solar Collector. *Energies* **2017**, *10*, 491. [CrossRef]
14. Sornek, K.; Filipowicz, M.; Jasek, J. The Use of Fresnel Lenses to Improve the Efficiency of Photovoltaic Modules for Building-integrated Concentrating Photovoltaic Systems. *J. Sustain. Dev. Energy Water Environ. Syst.* **2018**, *6*, 415–426. [CrossRef]
15. Renno, C.; Perone, A. Experimental modeling of the optical and energy performances of a point-focus CPV system applied to a residential user. *Energy* **2021**, *215*, 119156. [CrossRef]
16. Papis-Frączek, K.; Sornek, K. A Review on Heat Extraction Devices for CPVT Systems with Active Liquid Cooling. *Energies* **2022**, *15*, 6123. [CrossRef]
17. Figaj, R.; Żołądek, M. Experimental and numerical analysis of hybrid solar heating and cooling system for a residential user. *Renew Energy* **2021**, *172*, 955–967. [CrossRef]
18. Figaj, R.; Żołądek, M.; Homa, M.; Pałac, A. A Novel Hybrid Polygeneration System Based on Biomass, Wind and Solar Energy for Micro-Scale Isolated Communities. *Energies* **2022**, *15*, 6331. [CrossRef]
19. Garde, F.; Ayoub, J.; Aelenei, L.; Aelenei, D.; Scognamiglio, A. *Solution Sets for Net Zero Energy Buildings: Feedback from 30 Buildings Worldwide*; John Wiley & Sons: Hoboken, NJ, USA, 2017.
20. Hu, Z.; He, W.; Ji, J.; Zhang, S. A review on the application of Trombe wall system in buildings. *Renew. Sustain. Energy Rev.* **2017**, *70*, 976–987. [CrossRef]
21. Xu, W.; Guo, H.; Ma, C. An active solar water wall for passive solar greenhouse heating. *Appl. Energy* **2022**, *308*, 118270. [CrossRef]
22. Sharifi, A.; Yamagata, Y. Roof ponds as passive heating and cooling systems: A systematic review. *Appl. Energy* **2015**, *160*, 336–357. [CrossRef]
23. Szokolay, S.V. Passive Heating and Cooling. In *Sun Power (Second Edition): An Introduction to the Applications of Solar Energy*; Pergamon Press: Oxford, UK, 1983; Volume 3, pp. 113–131. [CrossRef]
24. Passive Solar Design—Sustainability n.d. Available online: https://sustainability.williams.edu/green-building-basics/passive-solar-design/ (accessed on 14 August 2022).
25. Wang, Q.; Zhang, G.; Wu, Q.; Li, W.; Shi, L. A combined wall and roof solar chimney in one building. *Energy* **2022**, *240*, 122480. [CrossRef]
26. Fang, Z.; Wang, W.; Chen, Y.; Song, J. Structural and Heat Transfer Model Analysis of Wall-Mounted Solar Chimney Inlets and Outlets in Single-Story Buildings. *Buildings* **2022**, *12*, 1790. [CrossRef]
27. Ahmed, O.K. Recent Advances in Photovoltaic-Trombe Wall System: A Review. In *Renewable Energy—Technologies and Applications*; IntechOpen: London, UK, 2020. [CrossRef]
28. Xiong, Q.; Alshehri, H.M.; Monfaredi, R.; Tayebi, T.; Majdoub, F.; Hajjar, A.; Delpisheh, M.; Izadi, M. Application of phase change material in improving trombe wall efficiency: An up-to-date and comprehensive overview. *Energy Build.* **2022**, *258*, 111824. [CrossRef]
29. Quesada, G.; Rousse, D.; Dutil, Y.; Badache, M.; Hallé, S. A comprehensive review of solar facades. Opaque solar facades. *Renew. Sustain. Energy Rev.* **2012**, *16*, 2820–2832. [CrossRef]

30. Brito-Coimbra, S.; Aelenei, D.; Gomes, M.G.; Rodrigues, A.M. Building Façade Retrofit with Solar Passive Technologies: A Literature Review. *Energies* **2021**, *14*, 1774. [CrossRef]
31. Dabaieh, M.; Elbably, A. Ventilated Trombe wall as a passive solar heating and cooling retrofitting approach; a low-tech design for off-grid settlements in semi-arid climates. *Sol. Energy* **2015**, *122*, 820–833. [CrossRef]
32. Tenpierik, M.; Wattez, Y.; Turrin, M.; Cosmatu, T.; Tsafou, S. Temperature Control in (Translucent) Phase Change Materials Applied in Facades: A Numerical Study. *Energies* **2019**, *12*, 3286. [CrossRef]
33. Li, S.; Zhu, N.; Hu, P.; Lei, F.; Deng, R. Numerical study on thermal performance of PCM Trombe Wall. *Energy Procedia* **2019**, *158*, 2441–2447. [CrossRef]
34. Parekh, V. Passive solar building. *International J. Appl. Eng. Res.* **2014**, *9*, 351–355. [CrossRef]
35. Soo, X.Y.D.; Png, Z.M.; Chua, M.H.; Yeo, J.C.C.; Ong, P.J.; Wang, S.; Wang, X.; Suwardi, A.; Cao, J.; Chen, Y.; et al. A highly flexible form-stable silicone-octadecane PCM composite for heat harvesting. *Mater. Today Adv.* **2022**, *14*, 100227. [CrossRef]
36. Shah, K.W.; Ong, P.J.; Chua, M.H.; Toh, S.H.G.; Lee, J.J.C.; Soo, X.Y.D.; Png, Z.M.; Ji, R.; Xu, J.; Zhu, Q. Application of phase change materials in building components and the use of nanotechnology for its improvement. *Energy Build.* **2022**, *262*, 112018. [CrossRef]
37. Abdullah, A.; Atallah, F.S.; Algburi, S.; Ahmed, O.K. Impact of a reflective mirrors on photovoltaic/trombe wall performance: Experimental assessment. *Results Eng.* **2022**, *16*, 100706. [CrossRef]
38. Omara, A.; Abuelnuor, A. Trombe walls with phase change materials: A review. *Energy Storage* **2020**, *2*, e123. [CrossRef]
39. Maghrabie, H.M.; Abdelkareem, M.A.; Elsaid, K.; Sayed, E.T.; Radwan, A.; Rezk, H.; Wilberforce, T.; Abo-Khalil, A.G.; Olabi, A. A review of solar chimney for natural ventilation of residential and non-residential buildings. *Sustain. Energy Technol. Assess.* **2022**, *52*, 102082. [CrossRef]
40. Layeni, A.T.; Waheed, M.A.; Adewumi, B.A.; Nwaokocha, C.N.; Sharifpur, M.; Tongo, S.O.; Okeze, R.C.; Mboreha, C.A. Computational and sensitivity analysis of a dual purpose solar chimney for buildings. *Mater. Today Proc.* **2021**, *47*, 4126–4136. [CrossRef]
41. Vargas-López, R.; Xamán, J.; Hernández-Pérez, I.; Arce, J.; Zavala-Guillén, I.; Jiménez, M.; Heras, M. Mathematical models of solar chimneys with a phase change material for ventilation of buildings: A review using global energy balance. *Energy* **2019**, *170*, 683–708. [CrossRef]
42. Berdowska, S. Analysis of the All-Year Operation of the Solar Chimney in Polish Climatic Conditions. *Energies* **2022**, *15*, 4738. [CrossRef]
43. Villar-Ramos, M.; Macias-Melo, E.; Aguilar-Castro, K.; Hernández-Pérez, I.; Arce, J.; Serrano-Arellano, J.; Díaz-Hernández, H.; López-Manrique, L. Parametric analysis of the thermal behavior of a single-channel solar chimney. *Sol. Energy* **2020**, *209*, 602–617. [CrossRef]
44. Hosien, M.; Selim, S. Effects of the geometrical and operational parameters and alternative outer cover materials on the performance of solar chimney used for natural ventilation. *Energy Build.* **2017**, *138*, 355–367. [CrossRef]
45. Shi, L.; Zhang, G.; Yang, W.; Huang, D.; Cheng, X.; Setunge, S. Determining the influencing factors on the performance of solar chimney in buildings. *Renew. Sustain. Energy Rev.* **2018**, *88*, 223–238. [CrossRef]
46. Zhang, H.; Tao, Y.; Nguyen, K.; Han, F.; Li, J.; Shi, L. A wall solar chimney to ventilate multi-zone buildings. *Sustain. Energy Technol. Assess.* **2021**, *47*, 101381. [CrossRef]
47. Cheng, X.; Shi, L.; Dai, P.; Zhang, G.; Yang, H.; Li, J. Study on optimizing design of solar chimney for natural ventilation and smoke exhaustion. *Energy Build.* **2018**, *170*, 145–156. [CrossRef]
48. Al-Kayiem, H.H.; Sreejaya, K.; Chikere, A.O. Experimental and numerical analysis of the influence of inlet configuration on the performance of a roof top solar chimney. *Energy Build.* **2018**, *159*, 89–98. [CrossRef]
49. Wang, Q.; Lai, J.; Claesen, L.; Yang, Z.; Lei, L.; Liu, W. A novel feature representation: Aggregating convolution kernels for image retrieval. *Neural Netw.* **2020**, *130*, 1–10. [CrossRef] [PubMed]
50. Zha, X.; Zhang, J.; Qin, M. Experimental and Numerical Studies of Solar Chimney for Ventilation in Low Energy Buildings. *Procedia Eng.* **2017**, *205*, 1612–1619. [CrossRef]
51. Sivalakshmi, S.; Raja, M.; Mahudeswaran, R.; Gowtham, G. Thermal performance of wall solar chimney integrated with a room under warm and humid conditions. *Mater. Today Proc.* **2021**, *43*, 1892–1895. [CrossRef]
52. Dordelly, J.C.F.; El Mankibi, M.; Roccamena, L.; Remion, G.; Landa, J.A. Experimental analysis of a PCM integrated solar chimney under laboratory conditions. *Sol. Energy* **2019**, *188*, 1332–1348. [CrossRef]
53. Shi, L. Theoretical models for wall solar chimney under cooling and heating modes considering room configuration. *Energy* **2018**, *165*, 925–938. [CrossRef]
54. Nguyen, Y.; Wells, J. A numerical study on induced flowrate and thermal efficiency of a solar chimney with horizontal absorber surface for ventilation of buildings. *J. Build. Eng.* **2020**, *28*, 101050. [CrossRef]
55. Shaari, A.M.; Abdullah, K.; Batcha, M.F.M.; Salleh, H.; Wae-Hayee, M. Effect of Converging Duct on Solar Chimney. *CFD Lett.* **2020**, *12*, 89–97. [CrossRef]
56. Moosavi, L.; Zandi, M.; Bidi, M.; Behroozizade, E.; Kazemi, I. New design for solar chimney with integrated windcatcher for space cooling and ventilation. *Build Env.* **2020**, *181*, 106785. [CrossRef]
57. Suhendri, S.; Hu, M.; Su, Y.; Darkwa, J.; Riffat, S. Performance evaluation of combined solar chimney and radiative cooling ventilation. *Build Env.* **2022**, *209*, 108686. [CrossRef]

58. Tao, Y.; Fang, X.; Setunge, S.; Tu, J.; Liu, J.; Shi, L. Naturally ventilated double-skin façade with adjustable louvers. *Sol. Energy* **2021**, *225*, 33–43. [CrossRef]
59. He, G.; Lv, D. Distributed heat absorption in a solar chimney to enhance ventilation. *Sol. Energy* **2022**, *238*, 315–326. [CrossRef]
60. Hweij, W.A.; Al Touma, A.; Ghali, K.; Ghaddar, N. Evaporatively-cooled window driven by solar chimney to improve energy efficiency and thermal comfort in dry desert climate. *Energy Build.* **2017**, *139*, 755–761. [CrossRef]
61. Salehi, A.; Fayaz, R.; Bozorgi, M.; Asadi, S.; Costanzo, V.; Imani, N.; Nocera, F. Investigation of thermal comfort efficacy of solar chimneys under different climates and operation time periods. *Energy Build.* **2019**, *205*, 109528. [CrossRef]
62. Nateghi, S.; Jahangir, M.H. Performance evaluation of solar chimneys in providing the thermal comfort range of the building using phase change materials. *Clean. Mater.* **2022**, *5*, 100120. [CrossRef]
63. Al Touma, A.; Ghali, K.; Ghaddar, N.; Ismail, N. Solar chimney integrated with passive evaporative cooler applied on glazing surfaces. *Energy* **2016**, *115*, 169–179. [CrossRef]
64. Fidaros, D.; Baxevanou, C.; Markousi, M.; Tsangrassoulis, A. Assessment of Various Trombe Wall Geometries with CFD Study. *Sustainability* **2022**, *14*, 4877. [CrossRef]
65. Chen, H.; Liu, S.; Eftekhari, M.; Li, Y.; Ji, W.; Shen, Y. Experimental studies on the energy performance of a novel wavy-shape Trombe wall. *J. Build. Eng.* **2022**, *61*, 105242. [CrossRef]
66. Owczarek, M. Thermal Fluxes and Solar Energy Storage in a Massive Brick Wall in Natural Conditions. *Energies* **2021**, *14*, 8093. [CrossRef]
67. Błotny, J.; Nemś, M. Analysis of the Impact of the Construction of a Trombe Wall on the Thermal Comfort in a Building Located in Wrocław, Poland. *Atmosphere* **2019**, *10*, 761. [CrossRef]
68. Zhu, Y.; Zhang, T.; Ma, Q.; Fukuda, H. Thermal Performance and Optimizing of Composite Trombe Wall with Temperature-Controlled DC Fan in Winter. *Sustainability* **2022**, *14*, 3080. [CrossRef]
69. Ma, Q.; Fukuda, H.; Kobatake, T.; Lee, M. Study of a Double-Layer Trombe Wall Assisted by a Temperature-Controlled DC Fan for Heating Seasons. *Sustainability* **2017**, *9*, 2179. [CrossRef]
70. Lohmann, V.; Santos, P. Trombe Wall Thermal Behavior and Energy Efficiency of a Light Steel Frame Compartment: Experimental and Numerical Assessments. *Energies* **2020**, *13*, 2744. [CrossRef]
71. MISIK, P.; Krasoń, J. Thermal Efficiency of Trombe Wall in the South Facade of a Frame Building. *Energies* **2021**, *14*, 580. [CrossRef]
72. Kostikov, S.A.; Yiqiang, J.; Grinkrug, N.V. Employment of a Trombe wall in Modern Heating Systems. In *IOP Conference Series: Materials Science and Engineering*; IOP Publishing: Bristol, UK, 2020; Volume 753, p. 022017. [CrossRef]
73. Kostikov, S.; Grinkrug, M.; Yiqiang, J. Comparative technical and economic analysis of the Trombe wall use in the heat supply system at different climatic conditions. *J. Phys. Conf. Ser.* **2020**, *1614*, 012064. [CrossRef]
74. Mohamad, A.; Taler, J.; Ocłoń, P. Trombe Wall Utilization for Cold and Hot Climate Conditions. *Energies* **2019**, *12*, 285. [CrossRef]
75. Li, J.; Zhang, Y.; Zhu, Z.; Zhu, J.; Luo, J.; Peng, F.; Sun, X. Thermal comfort in a building with Trombe wall integrated with phase change materials in hot summer and cold winter region without air conditioning. *Energy Built. Environ.* 2022; *in press*. [CrossRef]
76. Sornek, K.; Papis-Frączek, K. Development and Tests of the Solar Air Heater with Thermal Energy Storage. *Energies* **2022**, *15*, 6583. [CrossRef]
77. Özdenefe, M.; Atikol, U.; Rezaei, M. Trombe wall size-determination based on economic and thermal comfort viability. *Sol. Energy* **2018**, *174*, 359–372. [CrossRef]
78. Bojić, M.; Johannes, K.; Kuznik, F. Optimizing energy and environmental performance of passive Trombe wall. *Energy Build.* **2014**, *70*, 279–286. [CrossRef]
79. Zhang, H.; Shu, H. A Comprehensive Evaluation on Energy, Economic and Environmental Performance of the Trombe Wall during the Heating Season. *J. Therm. Sci.* **2019**, *28*, 1141–1149. [CrossRef]
80. Stazi, F.; Mastrucci, A.; Munafò, P. Life cycle assessment approach for the optimization of sustainable building envelopes: An application on solar wall systems. *Build Env.* **2012**, *58*, 278–288. [CrossRef]
81. Rehman, A.; Sheikh, S.; Kausar, Z.; McCormack, S. Numerical Simulation of a Novel Dual Layered Phase Change Material Brick Wall for Human Comfort in Hot and Cold Climatic Conditions. *Energies* **2021**, *14*, 4032. [CrossRef]
82. Rehman, A.; Ghafoor, N.; Sheikh, S.; Kausar, Z.; Rauf, F.; Sher, F.; Shah, M.; Yaqoob, H. A Study of Hot Climate Low-Cost Low-Energy Eco-Friendly Building Envelope with Embedded Phase Change Material. *Energies* **2021**, *14*, 3544. [CrossRef]
83. Leang, E.; Tittelein, P.; Zalewski, L.; Lassue, S. Impact of a Composite Trombe Wall Incorporating Phase Change Materials on the Thermal Behavior of an Individual House with Low Energy Consumption. *Energies* **2020**, *13*, 4872. [CrossRef]
84. Lichołai, L.; Starakiewicz, A.; Krasoń, J.; Miąsik, P. The Influence of Glazing on the Functioning of a Trombe Wall Containing a Phase Change Material. *Energies* **2021**, *14*, 5243. [CrossRef]
85. Yang, L.; Dhahad, H.A.; Chen, M.; Huang, Z.; Anqi, A.E.; Rajhi, A.A.; Qader, D.N. Transient analysis of buildings with Trombe wall in a southern envelope and strengthening efficacy by adding phase change material. *J. Build. Eng.* **2022**, *55*, 104670. [CrossRef]
86. Sanchez, P.F.; Hancco, L.M. Trombe walls with porous medium insertion and their influence on thermal comfort in flats in Cusco, Peru. *Energy Built. Environ.* 2022; *in press*. [CrossRef]
87. Saboori, T.; Zhao, L.; Mesgarpour, M.; Wongwises, S.; Mahian, O. A novel macro-scale machine learning prediction based on high-fidelity CFD simulations: A case study on the pore-scale porous Trombe wall with phase change material capsulation. *J. Build. Eng.* **2022**, *54*, 104505. [CrossRef]

88. Simões, N.; Manaia, M.; Simões, I. Energy performance of solar and Trombe walls in Mediterranean climates. *Energy* **2021**, *234*, 121197. [CrossRef]
89. Mabrouki, A.; Karim, Y.B.; Hassani, H.O.; Jamali, Y.; Khaldoun, A. A study of a passive heating design employing a Trombe wall with PCM: A numerical investigation of the semi-oceanic climate in Morocco. *Mater. Today Proc.* **2022**, *72*, 3626–3631. [CrossRef]
90. Zhu, N.; Deng, R.; Hu, P.; Lei, F.; Xu, L.; Jiang, Z. Coupling optimization study of key influencing factors on PCM trombe wall for year thermal management. *Energy* **2021**, *236*, 121470. [CrossRef]
91. Fateh, A.; Borelli, D.; Devia, F.; Weinläder, H. Summer thermal performances of PCM-integrated insulation layers for light-weight building walls: Effect of orientation and melting point temperature. *Therm. Sci. Eng. Prog.* **2018**, *6*, 361–369. [CrossRef]
92. Tlili, I.; Alharbi, T. Investigation into the effect of changing the size of the air quality and stream to the trombe wall for two different arrangements of rectangular blocks of phase change material in this wall. *J. Build. Eng.* **2022**, *52*, 104328. [CrossRef]
93. Seyhan, A.K.; Kara, Y.A. Energy and Environmental Evaluation of a PCM Wall Covered with Novel Triple Glass. *Omer Halisdemir Univ. J. Eng. Sci.* **2018**, *7*, 306–315. [CrossRef]
94. Zhu, Q.; Chua, M.H.; Ong, P.J.; Lee, J.J.C.; Chin, K.L.O.; Wang, S.; Kai, D.; Ji, R.; Kong, J.; Dong, Z.; et al. Recent advances in nanotechnology-based functional coatings for the built environment. *Mater. Today Adv.* **2022**, *15*, 100270. [CrossRef]
95. Soo, X.Y.D.; Muiruri, J.K.; Yeo, J.C.C.; Png, Z.M.; Sng, A.; Xie, H.; Ji, R.; Wang, S.; Liu, H.; Xu, J.; et al. Polyethylene glycol/polylactic acid block co-polymers as solid–solid phase change materials. *SmartMat* **2023**, e1188. [CrossRef]
96. Lin, Y.; Ji, J.; Zhou, F.; Ma, Y.; Luo, K.; Lu, X. Experimental and numerical study on the performance of a built-middle PV Trombe wall system. *Energy Build.* **2019**, *200*, 47–57. [CrossRef]
97. Hu, Z.; He, W.; Hu, D.; Lv, S.; Wang, L.; Ji, J.; Chen, H.; Ma, J. Design, construction and performance testing of a PV blind-integrated Trombe wall module. *Appl. Energy* **2017**, *203*, 643–656. [CrossRef]
98. Hu, Z.; He, W.; Ji, J.; Hu, D.; Lv, S.; Chen, H.; Shen, Z. Comparative study on the annual performance of three types of building integrated photovoltaic (BIPV) Trombe wall system. *Appl. Energy* **2017**, *194*, 81–93. [CrossRef]
99. Islam, N.; Irshad, K.; Zahir, H.; Islam, S. Numerical and experimental study on the performance of a Photovoltaic Trombe wall system with Venetian blinds. *Energy* **2021**, *218*, 119542. [CrossRef]
100. Irshad, K.; Algarni, S.; Islam, N.; Rehman, S.; Zahir, H.; Pasha, A.A.; Pillai, S.N. Parametric analysis and optimization of a novel photovoltaic trombe wall system with venetian blinds: Experimental and computational study. *Case Stud. Therm. Eng.* **2022**, *34*, 101958. [CrossRef]
101. Bruno, R.; Bevilacqua, P.; Cirone, D.; Perrella, S.; Rollo, A. A Calibration of the Solar Load Ratio Method to Determine the Heat Gain in PV-Trombe Walls. *Energies* **2022**, *15*, 328. [CrossRef]
102. Zhao, O.; Zhang, W.; Chen, M.; Xie, L.; Li, J.; Li, Z.; Zhong, J.; Wu, X. Experimental and Numerical Study on the Performance of Innovative Bifacial Photovoltaic Wall System. *Sustain. Cities Soc.* **2022**, *85*, 104085. [CrossRef]
103. Abed, A.A.; Ahmed, O.K.; Weis, M.M.; Ali, Z.H. Influence of glass cover on the characteristics of PV/trombe wall with BI-fluid cooling. *Case Stud. Therm. Eng.* **2021**, *27*, 101273. [CrossRef]
104. Abdullah, A.A.; Attulla, F.S.; Ahmed, O.K.; Algburi, S. Effect of cooling method on the performance of PV/Trombe wall: Experimental assessment. *Therm. Sci. Eng. Prog.* **2022**, *30*, 101273. [CrossRef]
105. Luo, Y.; Zhang, L.; Liu, Z.; Wu, J.; Zhang, Y.; Wu, Z. Numerical evaluation on energy saving potential of a solar photovoltaic thermoelectric radiant wall system in cooling dominant climates. *Energy* **2018**, *142*, 384–399. [CrossRef]
106. Abdullah, A.A.; Atallah, F.S.; Ahmed, O.K.; Daoud, R.W. Performance improvement of photovoltaic/Trombe wall by using phase change material: Experimental assessment. *J. Energy Storage* **2022**, *55*, 105596. [CrossRef]
107. Yu, B.; Liu, X.; Li, N.; Liu, S.; Ji, J. The performance analysis of a purified PV/T-Trombe wall based on thermal catalytic oxidation process in winter. *Energy Convers. Manag.* **2020**, *203*, 112262. [CrossRef]
108. Wu, S.-Y.; Xu, L.; Xiao, L. Performance study of a novel multi-functional Trombe wall with air purification, photovoltaic, heating and ventilation. *Energy Convers. Manag.* **2020**, *203*, 112229. [CrossRef]